

Nanoscale

Accepted Manuscript



This is an *Accepted Manuscript*, which has been through the Royal Society of Chemistry peer review process and has been accepted for publication.

Accepted Manuscripts are published online shortly after acceptance, before technical editing, formatting and proof reading. Using this free service, authors can make their results available to the community, in citable form, before we publish the edited article. We will replace this *Accepted Manuscript* with the edited and formatted *Advance Article* as soon as it is available.

You can find more information about *Accepted Manuscripts* in the [Information for Authors](#).

Please note that technical editing may introduce minor changes to the text and/or graphics, which may alter content. The journal's standard [Terms & Conditions](#) and the [Ethical guidelines](#) still apply. In no event shall the Royal Society of Chemistry be held responsible for any errors or omissions in this *Accepted Manuscript* or any consequences arising from the use of any information it contains.

Critical Factors of the 3D Microstructural Formation in Hybrid Conductive Adhesive Materials by X-ray Nano-tomography

Yu-chen Karen Chen-Wiegar¹, Miriam Figueroa^{1,2}, Stanislas Petrash³, Jose Garcia-Miralles³, Jun Wang^{1*}

¹ Photon Sciences Directorate Brookhaven National Laboratory, Upton, NY, 11973, USA

² Department of Mechanical Engineering, University of Puerto Rico, Mayaguez Campus, Mayaguez, PR, 00681, Puerto Rico

³ Henkel Corporation, Bridgewater, NJ, 08807, USA

* Corresponding author: Jun Wang, phone: 631 344-2661, fax 631 344-3238 and email: junwang@bnl.gov

Abstract

Conductive adhesives are found favorable in a wide range of applications including lead-free solder in micro-chip, flexible and printable electronics and enhancing performance for energy storage devices. Composite materials which comprise metallic fillers and polymer matrix are of great interests to be implemented as hybrid conductive adhesives. Here we investigated a cost-effective conductive adhesive material consist of silver-coated copper a micro-fillers using synchrotron-based three-dimensional (3D) x-ray nano-tomography. The key factors of affecting the quality and the performance of the material were quantitatively studied in 3D at nanometer scale for the first time. A critical characteristic parameter, defined as a shape-factor, was determined to yield high quality silver coating leading to satisfying performance. A 'stack-and-screen' mechanism was

proposed to elaborate such a phenomenon. The findings and the technique developed in this work will facilitate the future advancement of conductive adhesives to bring great impact in micro-electronics and other applications.

Key Words: Conductive adhesives, hybrid adhesives, x-ray nano-tomography, 3D imaging, 3D quantitative analysis, TXM

Text

Modern computers and advanced electronics drive the high demand for a lead-free solder to replace the widely used tin-lead alloy, which provides connection from one circuit element to another¹. Hybrid electronically conductive adhesives comprised of a polymer matrix and conductive fillers hold a great promise to achieve such a goal² with many advantages: they are more environmentally friendly, can be processed at lower temperature, can be mass-produced more simply with a faster rate via screen-printing and roll printing, exhibit lower stress on the substrate, and can be printed with higher spatial resolution³. In recent years, emerging technologies in flexible and printed electronics have further driven innovation in conductive adhesive materials sought for their flexible nature^{4,5}. Despite their promise, the cost and the performance of conductive fillers need to be improved to meet the global economic demands. Metallic fillers play a critical role in conductive adhesives, providing the conductive pathway and therefore determining the conductivity of the adhesives. Their size, shape and distribution within a matrix also affect the mechanical durability of the adhesives. In this work, an advanced conductive adhesive with economical Ag-Cu fillers was comprehensively and quantitatively characterized in three-dimensions (3D) by x-ray nano-tomography. A critical shape-

factor was found to enable a complete surface coverage during Ag deposition due to a 'stack-and-screen' mechanism. The results from this work provide important insight for better designing and engineering the processing of the advanced conductive adhesive materials, which have a grand economic impact for applications in electronics and flexible devices.

While gold (Au) and silver (Ag) micro-powders possess necessary properties as fillers for conductive adhesives, their wide applications have been limited because of the increasing price of these materials. Copper (Cu) is economical with excellent conductivity and can serve as an ideal alternative filler material for conductive adhesives. However, Cu oxidizes at relatively low temperature during the aging process and generates non-conductive oxidations, resulting in long-term reliability issues^{6, 7}. Recently, hybrid silver-coated copper fillers have emerged as a potentially promising solution to overcome the issues discussed above⁷. Copper micro-powders are coated with a thin layer of silver by electro-less plating⁸⁻¹⁰ to produce the fillers. Compared with alternative coating methods such as electroplating or deposition in vacuum, the electro-less plating method is superior in its fast coating rate. Nevertheless, it remains critical in such a method to better assess the quality of the Ag coating, which prevents the core Cu particles from being oxidized and losing conductivity under elevated temperature. When Ag is oxidized, the resulting silver oxides remain conductive and will therefore not compromise the performance of the adhesive. While the Ag surface coverage directly determines the performances and longevity of Ag-Cu fillers, it remains unclear what factors affect the results of Ag-coverage. The existing optimization process is based on trial-and-error process with minimum quantitative understanding of how to improve the

quality of the Ag coating. A direct 3D imaging with sub-50 nm resolution via synchrotron-based nano-tomography¹¹ and precise quantification of the hybrid adhesives were therefore carried out to address this missing information. The Cu particle size, Ag coating thickness and quality, particle segregation, and connectivity, along with the effects of the shape and size on the Ag coating coverage are presented and discussed.

The scanning electron microscope (SEM) image of focused ion beam (FIB) sections of resin filled with the Ag-coated Cu particles is shown in Figure 1(A). The damage to the structure of the resin and the filler from the FIB process is clearly visible. Most of the resin next to the cross-section appears to be disturbed along the path of the Gallium ion beam. Nevertheless, it shows that the silver coating appears to be thin and relatively uniform, and many particles are in contact to form conductive pathways. The edge of the particle in the cross-section is shown in the inset of the Figure 1(A). Next to the copper core we observe a layer of silver with darker inclusions, which could be copper oxides. The energy-dispersive x-ray spectroscopy results in Figure 1(B) show the distribution of the Cu core and Ag surface. While some insight can be gained from FIB-SEM, the information is limited to a small cross-section of the sample. The overall morphology of the sample and the quality of the coating is not fully accessible and a true 3D measurement is required.

With the experimental details provided in Appendix 1, Figure 1(C) shows a raw TXM projection of the conductive adhesive material sample with Ag-Cu micro-fillers from one angular position. An excellent imaging contrast between the surface Ag coating and the Cu particle was observed due to the difference in x-ray attenuation (as indicated

as arrows in the inserts). A full sample volume rendering from the tomographic reconstruction of the Ag-Cu adhesive is presented in Figure 1(D).

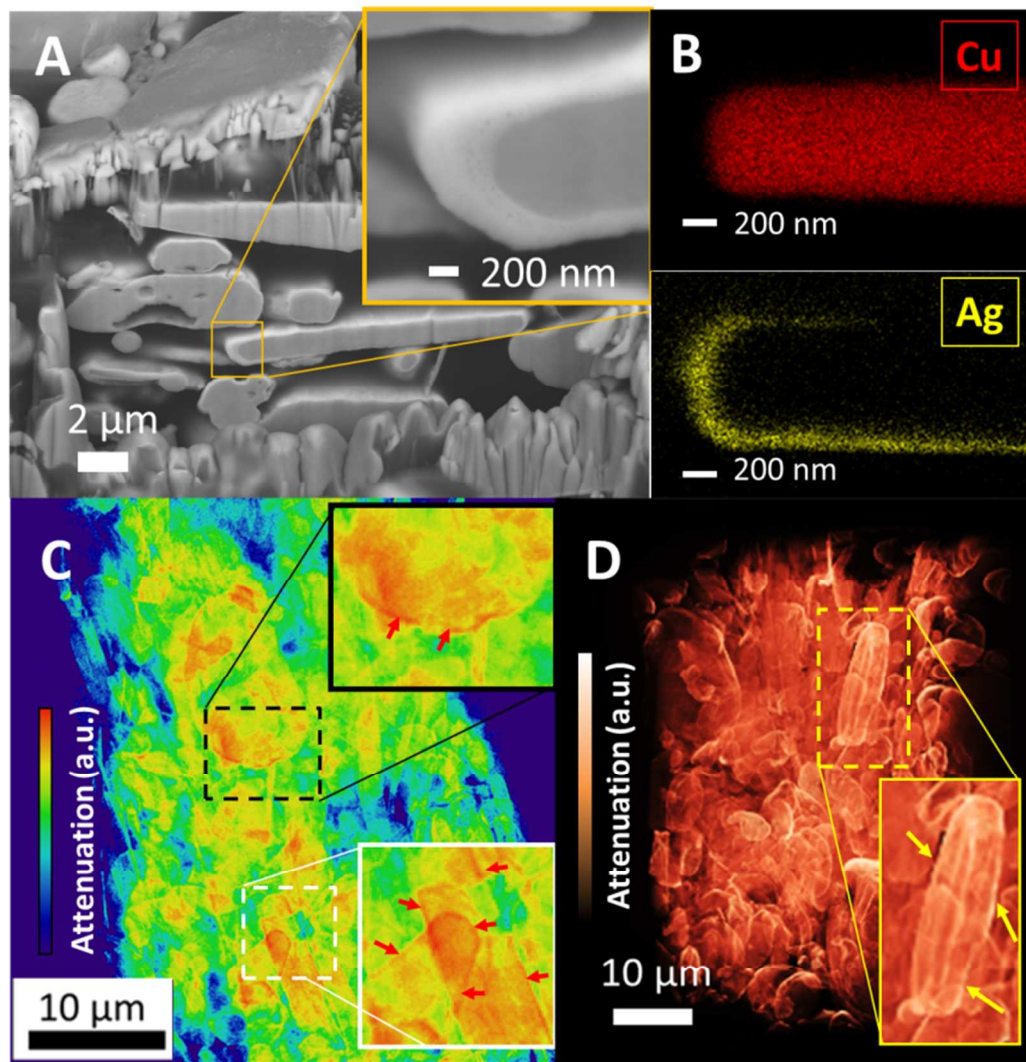


Figure 1 – Images of the conductive adhesive material sample with Ag-Cu micro-fillers characterized by TXM: (A) FIB-SEM cross-section showing the 3D morphology of the Ag-coated Cu particle, (B) EDX map of the Cu core and the Ag surface to verify the composition, (C) TXM projection from one angular position, and (D) TXM 3D reconstruction volume rendering for visualization.

A cross-section from the reconstruction of the TXM can be seen in Figure 2(A), where the attenuation coefficients were reconstructed via mathematical algorithm. The high contrast between Ag [red color in Figure 2(A)] and Cu (blue color) is critical, as it enables an accurate 3D quantification. This reconstructed volume was then segmented as shown in Figure 2(B) to separate the Ag surface coating from the Cu, where the 3D analysis was performed to quantify the morphology in order to understand the surface coating quality and its correlation with 3D parameters.

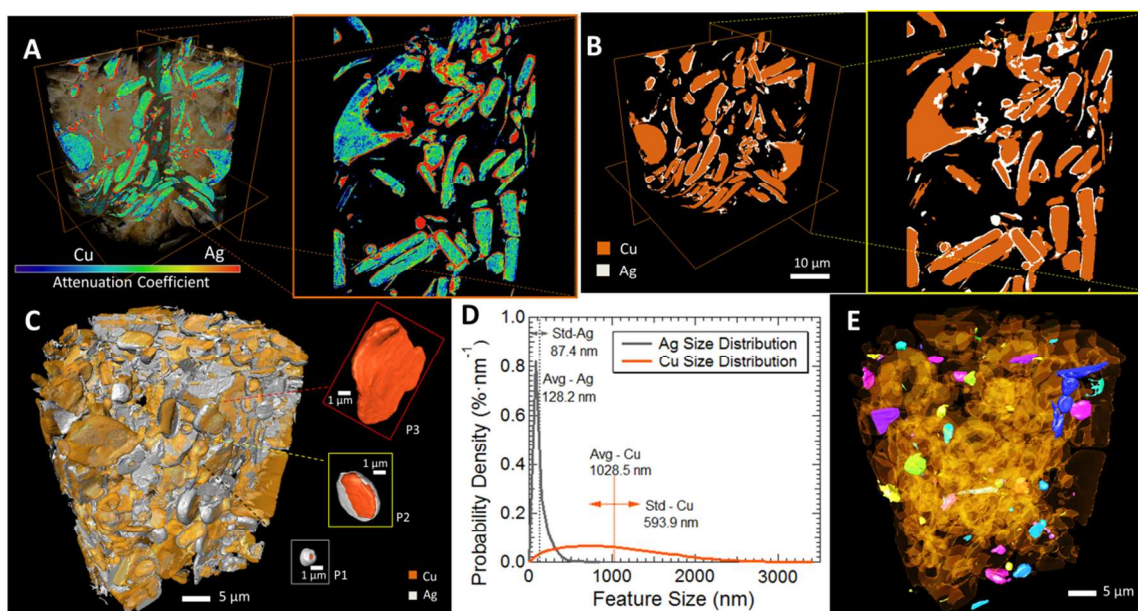


Figure 2 - Segmentation of reconstructed images and bulk statistics: (A) pseudo cross-section from TXM Reconstruction, (B) segmented results using Watershed segmentation to separate: Ag (white) Cu (orange) and the background, (C) 3D view of the segmented adhesives with Ag-coated Cu particle as fillers, (D) The size distribution, average size (Avg) and standard deviation (Std) of the Cu particle and Ag coating, and (E) 98.98%

particles are connected (yellow) with highlights of the isolated Ag-coated Cu particles (in various colors).

After segmentation, the Cu and Ag phases are entirely separated. The 3D view of the segmented volume can be found in Figure 2 (C). Figure 2 (D) shows the size distribution for the Cu particle and the Ag coating. A thickness variation of $128.2 \text{ nm} \pm 87.4 \text{ nm}$ was obtained for the Ag phase on Cu particles with an average diameter of $1028.5 \pm 593.9 \text{ nm}$. The particles exhibit an excellent connectivity of 98.97 vol%, as shown in the connected yellow network in Figure 2 (E). Only about 1 vol.% of the particles are isolated, which is shown in various colors in Figure 2 (E). This indicates that high conductivity can be achieved in these conductive adhesives materials.

However, the Ag coating coverage on Cu particles was measured to be only 38.79%. As a result, the surface of the Cu may be oxidized during the aging process or during operation when the temperature is elevated. The relatively low surface Ag coverage is no doubt harmful and indicates that the process to coat the Cu particle may be further improved. The detailed effects of the geometric parameters, including size and shape of the particles, are detailed below to provide guidelines to further improve the Ag coating coverage.

Four selected particles shown in the insets of Figure 2 (C) reveal the variation in particle size, shape, and surface coverage. The small round particle (P1) exhibits a nearly complete silver coverage of 97.76 % (surface %). A medium size, round particle (P2), shows a coverage of 74.48%. Finally, a large size particle (P3) exhibits 0% Ag coverage. The general trend seems to be that the larger the particle is, the lower the coverage will be.

An in-depth investigation with a new 3D analysis method we developed was performed to bring further insight into the relationship between the geometrical properties of the particle and the Ag coverage.

In order to obtain the correlation between particle size, shape and the Ag coverage, individual Cu particles were separated using algorithm available in Avizo, resulting in a total of 2339 particles. A visualization of the separate particles with various colors is shown in [Figure 3\(A\)](#). For each particle, three factors were calculated: its volume, shape factor, and surface coverage by Ag. In addition, the possibility of particle segregation was also examined. The segregation of the Ag-coated Cu particles in a resin matrix is undesired, because they will decrease the conductivity and corrosion performance of the final product. The segregation of particles will result in a spatial variation of the particle volume fraction. To quantify if the sample exhibited segregation, the volume fraction variation was studied by dividing the original volumes into smaller sub-volumes. The volume fraction of the hybrid fillers and the Ag coverage were quantified into $N \times N \times N$ independent volumes [see **Error! Reference source not found.**(A)]. In the final product, little relationship was found between volume fraction and surface coverage. This relationship is plotted in [Figure 3 \(B\)](#) with $N = 4-6$, and it implies a homogenous distribution of particle coverage in space during the processes of mixing the particles with the resin and aging. Though the particles might have been stacked during the deposition process, which could affect the coating ratio, the particles were well re-distributed during the later processes. The consistent average particle volume fraction shown in **Error! Reference source not found.**(B) further verifies this observation. Though the standard deviation increases with a smaller sampling volume,

the overall particle distribution was homogeneous and little segregation was observed. No stacking structure was observed in the final product, despite the strong correlation between the shape factor and the coverage shown previously. This demonstrates that the resin mixing process was able to release the aggregated particles to result in a homogeneous particle distribution. As a result, the sample will exhibit isotropic conductivity independent of sample location, and thus provide consistent performance.

The relationship between the particle size and the surface coverage is then quantified as shown in [Figure 3\(C\)](#). While some correlation can be observed in the figure, it is unclear if there is a direct correlation between the Cu particle size and the surface Ag coverage. A relationship between the particle sizes vs. the shape factor is shown in [Figure 3\(D\)](#). The shape factor directly represents if a particle is a ball or disk. A ball-shaped particle exhibits $S = 3$. For the disk shape, the S directly correlates to a particle's radius-to-thickness ratio (a), where the larger the shape factor, the higher the radius-to-thickness ratio will be, which means the disk is 'flatter'. It is important to state that the shape factor S solely depends on the shape of the particles and is completely independent from the size (volume or radius) of the particles. However, in [Figure 3\(D\)](#), there is a clear trend for the larger particle to exhibit a higher shape factor, which corresponds to a large radius-to-thickness ratio as in a disk shape case. An experimental relationship between the shape factor S and the particle volume was found to be $S = 11.06 - 23.41 V^{-0.066}$, loosely following a power relationship.

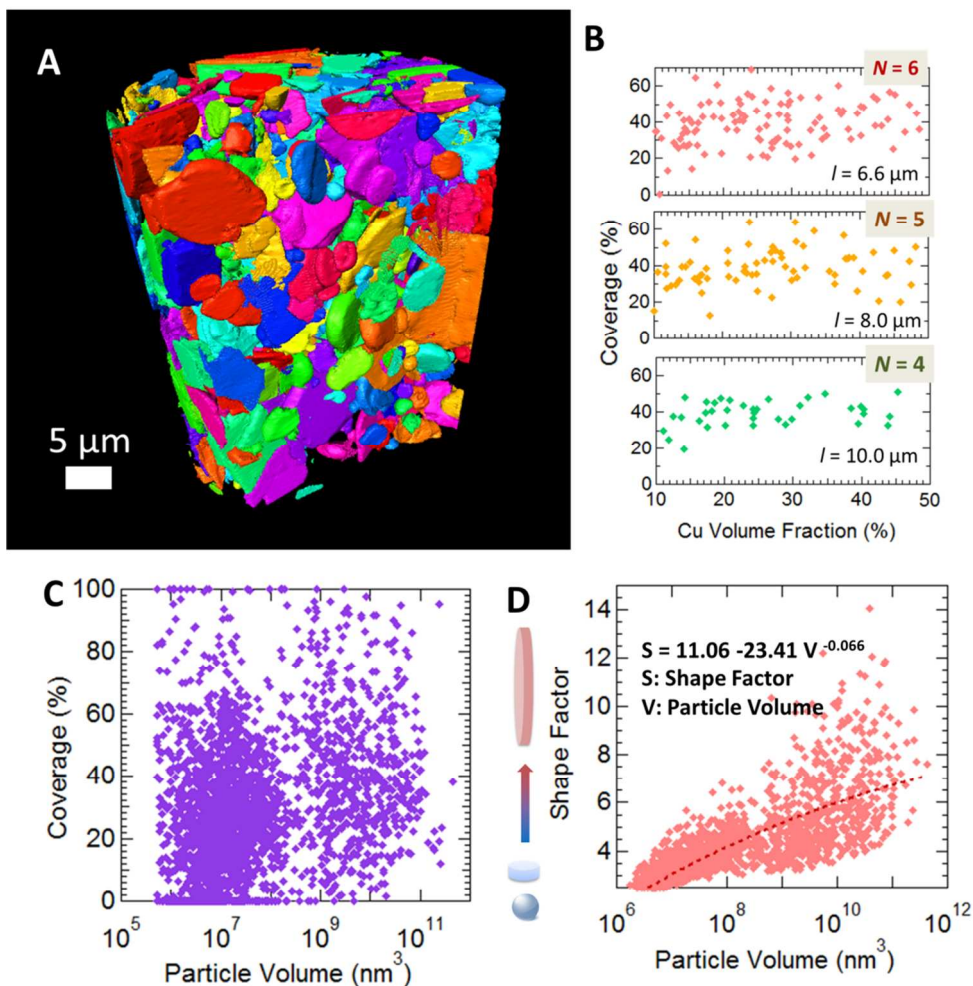


Figure 3 – Analysis of individual particles: (A) visualization of individual particles successfully separated in imaging processing, (B) Relationship between the Ag coverage and the particle volume fraction. The sub-volume length (l) = $40 \mu\text{m}/N$, (C) Scatter plot of the surface coverage vs particle volume, and (D) correlation between the shape factor vs. the particle volume.

While the size vs. coverage distribution shows a relatively randomized relationship, it is suspected that the shape factor might play a greater role in determining the Ag coverage on the Cu surface. A detailed analysis regarding the correlation between

the coverage vs. the shape factor can be found in Figure 4. First, Figure 4(A) shows a histogram of the particles categorized by their different shape factor. The sphere-shaped particles account for > 50% of the particles. However, due to their smaller size (as shown in [Figure 3(D)]), their surface area only accounts for ~1.86 % of the total surface area. A scatter plot of coverage vs shape factor is presented in Figure 4(B). There is a noticeable maximum coverage associate with each shape factor. The maximum coverage associated with each shape factor range is shown in Figure 4(C). Ball-shaped and disk-shaped particles with a small radius-to-thickness ratio can exhibit up to 100% surface coverage. However, once the shape factor exceeds a critical value, which is identified as 4.6, the maximum coverage can no longer be 100% but decreases as the shape factor increases. This critical shape factor corresponds to a radius-to-thickness ratio of 2.4. Once the radius of the disk of the particle is larger than 2.4 times of its thickness, the electro-less coating methods can no longer result in a full surface coverage of the Cu. The decrease of the maximum coverage against the shape factor follows a linear relationship of:

$$C_{max} = -0.087 S + 1.4 \quad [1],$$

where C_{max} is the maximum coverage and the S is the shape factor.

This also suggests that the inhomogeneous scatter plot shown in Figure 4 (B) might attribute mostly to the shape effects. See supplementary material for the discussion regarding the relationship between the average coverage vs. the shape factor.

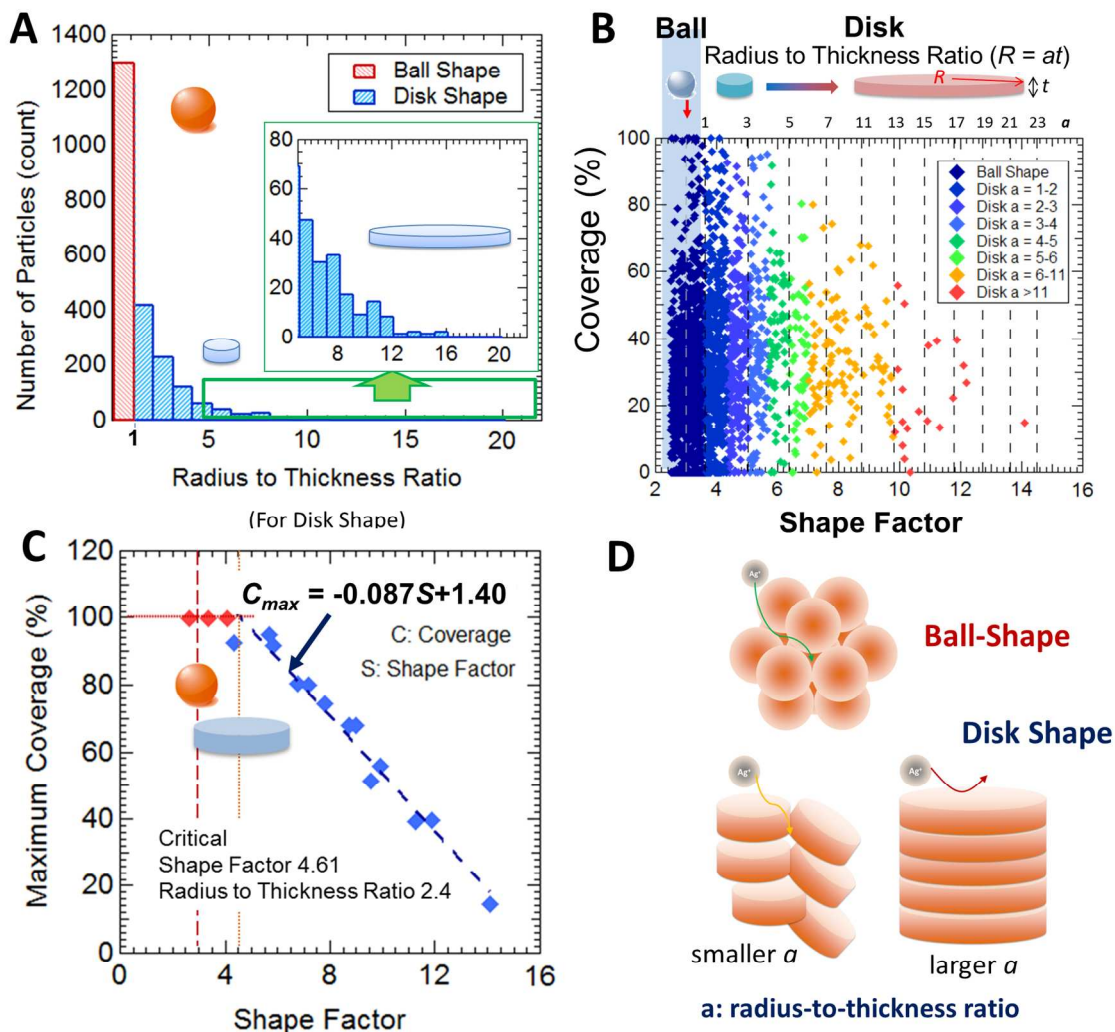


Figure 4 – Statistical summary of the relationship between the particle shape and the amount of Ag coverage: (A) histogram showing the particle number distribution among spherical shape and disk-shape with various radius-to-thickness ratio (a), (B) coverage vs. shape factor (defined to be independent of particle shape), (C) the maximum surface coverage vs. shape factor exhibits a critical shape factor of 4.61 ($a = 2.4$), above which the particles cannot be coated completely, and (D) mechanism of ‘stack and screen’ with the shape-determining maximum surface coverage.

It is believed that this critical radius-to-thickness effect results from the flatter particles having a higher tendency to “stack” during the silver deposition process. If several flat particles form a stack prior to or during the silver deposition process, they are effectively screening overlapping surfaces from the silver in the surrounding medium. Smaller particles will have much less tendency to aggregate and will therefore expose most of their surface to solution silver, leading to more uniform surface coverage. Spherical particles do not suffer from such stacking problems and therefore should exhibit the largest maximum coverage. An illustration that depicts this concept is shown in Figure 4 (E). The particles with spherical shapes, even with the closed-packed geometry (the closest packed geometry for spherical particles can still achieve 74% volume fraction), still exhibit only point contacts between particles. Therefore, ball-shaped particles allow sufficient diffusion during the electro-less plating process and the 100% surface coverage can be achieved. Disk particles with relatively low radius-to-volume ratios and smaller shape factors exhibit some ‘stack and screen’ problems, which result in lower surface coverage. In extreme cases, the disk particles with relatively high radius-to-volume ratios and larger shape factors exhibit the most severe ‘stack and screen’ problem and yield relatively low or nearly zero surface coverage. The shape factor and the radius-to-thickness parameter here are independent of the particle size and volume. Such stacks can then de-aggregate during the subsequent formulation stages, releasing “screened out” particles back into the mix. This ‘stack and screen’ problem therefore might be neglected because the end-product does not present such a stacking structure.

In conclusion, a comprehensive 3D morphological analysis was carried out on a conductive adhesive material with Ag-Cu hybrid micro-fillers. The critical 3D parameters that affect performance, including Ag coating coverage, the size of the Cu, the thickness of the Ag and its variation were quantified. The Ag coating thickness was quantified to be 128.2 ± 87.4 nm on Cu particles with an average diameter of 1028.5 ± 593.9 nm. The particles exhibit an excellent connectivity of 98.97 vol. %, where only ~ 1 vol% of the particles are isolated, indicating that high conductivity can be achieved in this ICA. Furthermore, the relationship between the particle size and shape was also established. The Ag coating over the Cu particles was determined to be 38.79%. This suggests that the process may be changed in order to improve the Ag coverage and hence the conductivity of the adhesive by yielding more ideal particle sizes and shapes. From the 3D analysis, spherical particles were shown to exhibit a maximum of 100 surf % of surface coverage. On the contrary, the disk-shaped particles with a radius-to-thickness larger than the critical 2.4 value cannot be fully coated. The maximum coverage was found to be linearly decreased with an increase of shape factor, which is independent of particle size. This may be due to a 'stacking-and-screening' mechanism during the electro-less plating process. Finally, the particle segregation found after the resin mixing and aging processes indicate that a homogenous particle distribution and isotropic performance were achieved. The x-ray nano-tomography was able to reveal morphological details and bring unique insights that were not accessible by other methods. This fact suggests that 3D morphological analysis on the images collected by x-ray nano-tomography is an efficient method to non-destructively analyze the conductive adhesive sample in three dimensions.

Reference

1. Y. Li, K. S. Moon and C. P. Wong, *Science*, 2005, **308**, 1419-1420.
2. M. A. Gaynes, R. H. Lewis, R. F. Saraf and J. M. Roldan, *Ieee Transactions on Components Packaging and Manufacturing Technology Part B-Advanced Packaging*, 1995, **18**, 299-304.
3. C. Yang, W. Lin, Z. Y. Li, R. W. Zhang, H. R. Wen, B. Gao, G. H. Chen, P. Gao, M. M. F. Yuen and C. P. Wong, *Adv. Funct. Mater.*, 2011, **21**, 4582-4588.
4. Z. Li, R. W. Zhang, K. S. Moon, Y. Liu, K. Hansen, T. R. Le and C. P. Wong, *Adv. Funct. Mater.*, 2013, **23**, 1459-1465.
5. A. C. Siegel, S. T. Phillips, M. D. Dickey, N. S. Lu, Z. G. Suo and G. M. Whitesides, *Adv. Funct. Mater.*, 2010, **20**, 28-35.
6. S. Y. Xu, D. A. Dillard and J. G. Dillard, *Int. J. Adhes. Adhes.*, 2003, **23**, 235-250.
7. X. R. Xu, X. J. Luo, H. R. Zhuang, W. L. Li and B. L. Zhang, *Mater. Lett.*, 2003, **57**, 3987-3991.
8. US4652465 A, 1987.
9. US5178909 A, 1993.
10. US5945158 A, 1999.
11. J. Wang, Y.-c. K. Chen, Q. Yuan, A. Tkachuk, C. Erdonmez, B. Hornberger and M. Feser, *Appl. Phys. Lett.*, 2012, **100**, 143107-143101-143104.